34th Annual International Conference of the IEEE EMBS
San Diego, California USA, 28 August - 1 September, 2012

Threshold Analysis of a Quasimonopolar Stimulation Paradigm in Visual Prosthesis

Paul. B. Matteucci* *Member, IEEE*, Spencer C. Chen*, *Member, IEEE,* Christopher Dodds*, *Member, IEEE,* Socrates DokosNigel, *Member, IEEE,* H. Lovell*, *Fellow, IEEE* and Gregg J. Suaning*, *Member, IEEE*

***Abstract* — The complexity of surgical implantation has always been a significant obstacle in the development of visual prosthetics. Implanting in the epi and sub-retinal spaces allows the prosthesis direct access to the retina, resulting in lower stimulation thresholds, potentially at the expense of robust mechanical stability and interface longevity. Implanting the stimulating electrode in the supra-choroidal space greatly simplifies surgery and improves mechanical stability. This is achieved at the cost of a higher activation threshold and reduced focus of the electric field at the target site of stimulation, given the increased distance between the stimulating electrodes and the target tissue. In order to contain the spread of the stimulating field, the authors proposed a hexagonal arrangement of return electrodes, at a further cost to the stimulation threshold over that of a monopolar stimulation paradigm. This study analyses the effect on activation thresholds of activating simultaneously the hexpolar guard electrodes and the distant monopolar return in what we have termed a quasimonopolar configuration. Results show that introducing a small element of monopolar stimulation significantly lowers the activation threshold otherwise required by a pure hexpolar return.**

I. Introduction

VISUAL neurostimulators have been at the forefront of implantable bionic technology due to the complexity of visual stimulation and the constraints introduced by the delicacy and dimensions of the eye.

With the proven success of pacemakers, deep brain stimulators and cochlear implants, to name a few, it is no wonder that various groups, attempting to restore some degree of sight to the visually impaired, utilize a wide range of techniques and technologies [1-7]. Approaches targeting the optic nerve [7] and directly the visual cortex [5, 8] are yielding intriguing results, however the main focus of researchers is electric stimulation of the retina which utilizes the remaining neural network of the eye that follows degenerative disease [1, 2, 3]. This is possible due to the fact that leading causes of blindness in developed nations, retinitis pigmentosa and age-related macular degeneration, cause a degeneration of the photoreceptors in the eye while leaving most of the remaining neuronal network virtually intact. Although several viable options exist, three main approaches are being pursued with regards to electrode positioning: epi-retinal[1, 3], sub-retinal [2] and supra-choroidal [9]. The epi-retinal approach involves complex surgery and the use of retinal tacks to hold the device in place [10]; this results in low mechanical stability but yields the closest proximity to the retinal ganglion cells and consequently the lowest stimulation thresholds [11]. Moreover, this approach cannot readily be applied in parallel with residual vision. The subretinal approach also requires complex and time-consuming surgery [2] with the danger of causing retinal detachment or tearing, however it also presents low thresholds due to the proximity to the target cells and the intimate contact of electrodes and tissue. Supra-choroidal devices can be implanted with a simplified surgical approach and places the electrode in a mechanically stable site between two, robust layers of tissue – the choroid and the sclera [9]. This however comes at the cost of higher stimulation thresholds due to the distance from the target cells and the electrical properties of the choroid.

When stimulating to a distant monopolar return, the increased distance from the target cells also results in an increased spread of the electric field. This spread can prove to be a deterrent in the choice of the otherwise advantageous supra-choroidal space, as it increases the complexity of achieving high density phosphene perceptions. In order to counteract this spread, the authors investigated hexpolar stimulation [12, 13]. Using this configuration the stimulation returns comprise six electrodes immediately surrounding the stimulating electrode rather than a distant, monopolar return. The resulting electric field is contained by the return electrodes, resulting in a more punctate stimulation on the retina, however at further expense of stimulation threshold owing to lateral shunting of the current.

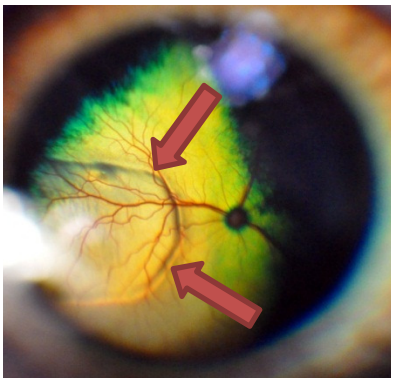

Figure 1 - Fundus image of a feline retina with the outline of the implanted retinal electrode clearly visible (arrows) due to distortion of the retina.

*Graduate School of Biomedical Engineering, University of New South Wales, Sydney, Australia.

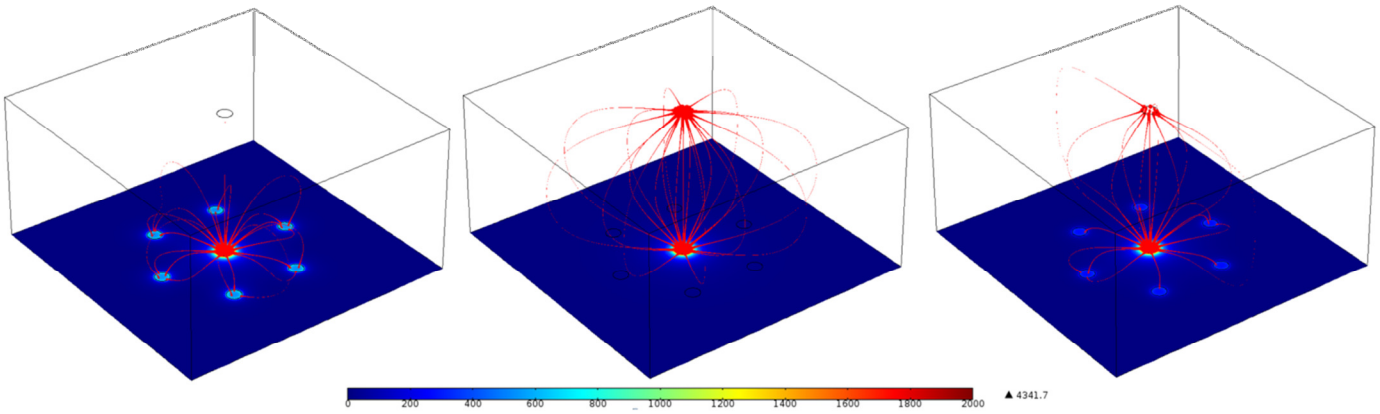

Figure 2 – Mathematical model of Quasimonopolar stimulation strategy (COMSOL Multiphysics). From left to right: pure hexpolar stimulation with the field contained but little vertical expansion; pure monopolar stimulation with high trans-retinal current flow and wide current spread; quasimonopolar stimulation with the overlapping monopolar and hexpolar fields. The lines represent the electrical field proportionally to the current intensity.

In this study the authors investigated the effect on thresholds of concurrently stimulating the hexagonal returns and a distant monopolar electrode, investigating the hypothesis that adding a monopolar element to a hexpolar stimulation will distort the hexpolar field towards the target tissue and result in lower thresholds.

II. Methodology

A. *Surgical Implantation*

A series of in vivo experiments were conducted on normally sighted cats (N = 2), with approval from the UNSW Ethics Committee. Acute experiments were performed over a period of three days.

Induction anaesthesia was achieved with a dose of ketamine (20 mg kg^{-1}) and xylazine (2mg kg^{-1}), anaesthesia was maintained using a constant infusion of Alfaxan (DOSAGE). During surgical setup, intra-venal and intra-arterial catheters were inserted for administration of pharmacological agents, and direct blood pressure measurement respectively. Respiration rate, CO_2 levels and core temperature were also monitored by means of a tracheal tube and rectally inserted thermal probe.

A 9 mm incision was made 4-5mm from the limbus and a pocket was created to accommodate the electrode. The stimulating electrode array was introduced and sutured into position. The resulting fundus image (Figure 1) taken immediately following surgery shows the outline of the array and its position relative to the optic disk. A craniotomy and durotomy in correspondence with the visual cortex were performed according to dimensions found in Tusa et al. [14]. The primary and secondary visual cortices were mapped utilising a platinum ball electrode and a custom, 32 channel surface electrode while stimulating the retina implant at a constant 400uA for 400us via the inserted array.

B. *Electrodes and Recording Devices*

A custom, 24 channel stimulating array was fabricated in-house. The Pt electrodes, arranged in a hexagonal mosaic were laser micromachined and surface roughened; they were fabricated on a silicon rubber substrate (MED-1000, Nusil, Carpenteria, California, USA) reinforced by a Dacron mesh (SH-21001-007, BioPlexus, California, USA). Once the cortical area of maximum response was located, a 100 channel (10x10) penetrating electrode array (Blackrock Microsystems, Utah, USA) was inserted.

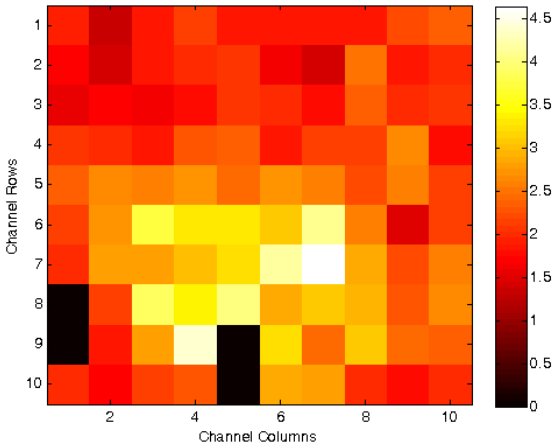

Figure 3 - Cortical activity as recorded from the penetrating electrode array showing focused activation in the area surrounding the "best cortical electrode" (see text). The colourbar on the right indicates cumulative spike counts over the 5-20ms window per stimulus

All recording electrodes were connected via 32 and 64 channel head stages (Tucker-Davis Technologies, Florida, USA) to a multi-channel amplifier (RZ2, Tucker-Davis Technologies, Florida, USA), through a 256 channel pre-amplifier (PZ2) unit by the same company. The resulting data was recorded onto a custom built Intel/Windows 64-bit desktop computer and processed offline using Matlab (The Mathworks, Inc, Massachusetts, USA).

To each step in this range, a second stimulation was overlaid, with an increasing amount of monopolar current, ranging from 0 to 160 µA in approximately 35 µA steps, while ensuring that at all times the charge per phase remained below 210 µC/cm^2 [15].

C. Stimulation Parameters and Offline Processing

The stimulation protocol was designed examine the effect of varying monopolar stimuli generated concurrently with the hexpolar stimulus.

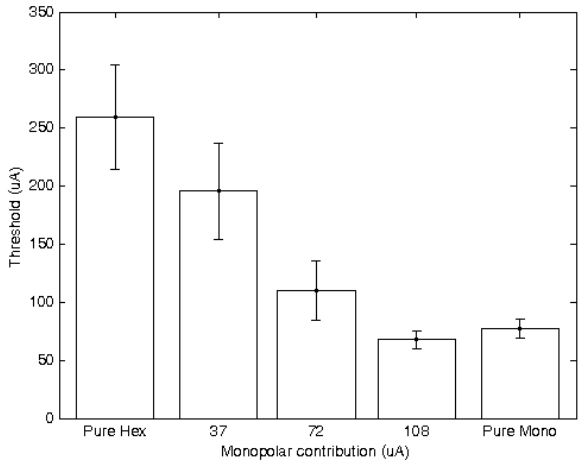

Figure 4 - Effect of the monopolar contribution on activation threshold. Error bars indicate the standard error (N=6 – explain (e.g. 2 eyes, etc.).

A hexpolar stimulus sequence was configured, consisting of 16 stimulation currents ranging from 0 to 650 μA in steps of approximately 35 μA.

The phase time was fixed at 500 μs, and either 25 or 50 repeats of each quasimonopolar current setting were recorded.

During offline processing, the raw recorded signal was first analysed and the 3 ms in correspondence with the stimulus artefact was removed in accordance with Fallon et al. [16].

The signal was then band pass filtered, passing a range of 300 Hz to 5000 Hz using a Butterworth 5th order filter.

The 100 ms preceding the stimulus onset of all stimuli were concatenated and the baseline RMS noise content within the signal calculated.

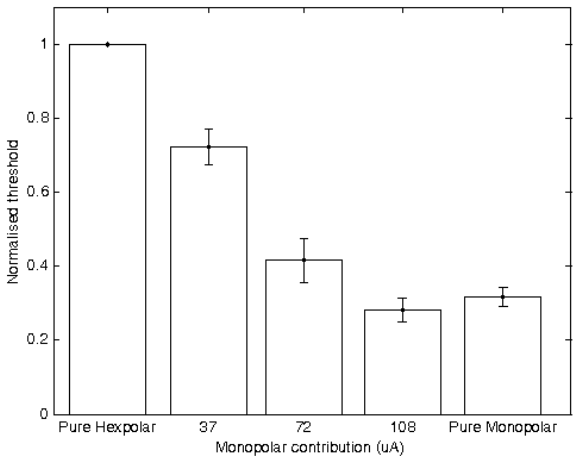

Figure 5 - The effect on threshold of increasing amounts of monopolar contribution normalised to pure hex theshold. Bars indicate the standard error (n=6 - explain).

The 3.4 or 3.6 times the RMS (depending on noise) was then used as a threshold to identify neural spikes. The spike quantities were then plotted relative to the cumulative current, and sigmoids fitted to this data. As an arbitrary indication of threshold, the p50 value from the fitted sigmoid was chosen.

D. Mathematical model

To compare the extent of electric field penetration into the retina under various quasimonopolar and monopolar stimulation modes, we implemented a 3D computational finite-element model of electric field distribution in a single hex electrode. The relevant equations were

$$\nabla.(-\sigma\nabla V) = 0$$
$$\mathbf{E} = \nabla V$$

where V is the electric potential and $\mathbf{E}$ is the electric field vector. A single hex electrode arrangement was implemented using COMSOL Multiphysics finite-element software 3-1 (COMSOL AB, Switzerland), a disc electrode of 200 μm diameter and center-center spacing of 1 mm. An anodic current of 100 μA was applied to the central electrode of this hex, and a user-specified fraction Q of this current was returned via a quasimonopolar ground return electrode, located 2 mm above the plane of the hex electrode (Figure 2). Conductivity of the volume was set to 1 S/m, similar to that of saline.

III. RESULTS

The experimental protocols designed were specifically aimed at determining the effect on activation threshold of combining monopolar and hexpolar stimulation and using a pure hexpolar threshold as an initial reference.

Localised cortical activity for hexpolar, monopolar and quasimonopolar stimulations was observed (Figure 3) in seven out of nine of the recording sites, so these seven recordings were chosen to evaluate threshold. Of these seven, one was discarded because of significant noise levels which resulted in skewed sigmoids and a clearly erroneous value for p50.

The cortical recordings were grouped based on the amount of monopolar current contributing to the quasimonopolar, which resulted in a spike count per channel of a range of quasimonopolar stimulations with a constant monopolar current and an increasing value of hexpolar.

The current increase in monopolar contribution (~36 μA) was determined by the limitations of the constant current stimulator used for these experiments; while the maximum amount of monopolar current used was determined by the fact that for current values above 108 μA, no value of hexpolar stimulation resulted in a sub-threshold stimulus, and therefore sigmoids could not be fitted.

The cumulative current (hexpolar + monopolar) used in the stimulation was used when plotting the sigmoids, so that the change in threshold could be observed. A pure monopolar recording was also included as part of the protocol to compare the levels of containment and activation threshold.

Figure 4 shows the recorded values for threshold for the six electrodes used to stimulate in the two experiments.

The large variation in threshold is likely due to the effect of electrode positioning. The recording electrode is inserted in correspondence with the maximum cortical activity for a single stimulating electrode; when the stimulating electrode is changed, larger activation is required for it to be detected in the original cortical site. Proximity to the fovea may also have an effect of recorded thresholds.

This variation can be excluded by normalising the threshold value by the maximum hexpolar threshold per recording site (

Figure **5**).

The results also indicate the effect of monopolar contributions on a hexpolar activation threshold to be exponential rather than linear.

IV. DISCUSSION

These results indicate that combining monopolar and hexpolar stimuli yields lower thresholds than using hexpolar alone. This appears to confirm the presence of monopolar and hexpolar fields around the electrodes, and superposition effect wherein higher charge density elicits action potentials for an overall significantly lower charge. When expressed in terms of percentage of the overall stimulation (Figure 5), it appears that the monopolar element has a more significant effect on the threshold than the hexpolar.

A potential drawback of hexpolar stimulation is the shunting which occurs in the plane of the stimulating electrode and the return electrodes (see for example the leftmost panel of Figure 2): this result in only the edges of the hexpolar electric field contributing directly to eliciting activation in the retina, resulting in high activation thresholds.

In contrast, the pure monopolar field flows from the stimulating electrode through the retina to the distant return, resulting in a less localised, but more efficient electrical stimulation circuit resulting in a lower threshold.

Comparing the threshold results with the modelling, the hypothesis of superposition of electrical fields appears to be confirmed. The areas of overlap of the two fields yield an area of charge density sufficiently high to elicit an activation, even though neither of the two fields would individually be sufficient for activation to occur.

If analysing these data independently, there would appear to be little reason to stimulate with quasimonopolar as it provides no direct benefit to the activation threshold, however, this analysis appears to confirm the modelling data. Further analysis will confirm if the low-threshold of monopolar can be combined with the high-focus field of hexpolar stimulation and the overlapping field can result in a high-focus, low threshold quasimonopolar stimulation strategy.

V. CONCLUSION

These results show promise in reducing high threshold levels, which exacerbate the difficulties associated with operating with hexpolar stimulation. By combining lowered threshold values with the charge containment properties of hexpolar stimulation, more efficacious and focused stimulations can be achieved by retinal implants, while maintaining the surgical simplicity and mechanical stability of the supra-choroidal space.

REFERENCES

[1] E. Zrenner, "The subretinal implant: can microphotodiode arrays replace degenerated retinal photoreceptors to restore vision?," *Ophthalmologica,* vol. 216 Suppl 1, pp. 8-20; discussion 52-3, 2002.

[2] D. B. Shire, S. K. Kelly, J. Chen, P. Doyle, M. D. Gingerich, S. F. Cogan, W. A. Drohan, O. Mendoza, L. Theogarajan, J. L. Wyatt, and J. F. Rizzo, "Development and implantation of a minimally invasive wireless subretinal neurostimulator," *IEEE Trans Biomed Eng,* vol. 56, pp. 2502-11, Oct 2009.

[3] D. Yanai, J. D. Weiland, M. Mahadevappa, R. J. Greenberg, I. Fine, and M. S. Humayun, "Visual performance using a retinal prosthesis in three subjects with retinitis pigmentosa," *American Journal of Ophthalmology,* vol. 143, pp. 820-827, May 2007.

[4] H. Gerding, F. P. Benner, and S. Taneri, "Experimental implantation of epiretinal retina implants (EPI-RET) with an IOL-type receiver unit," *J Neural Eng,* vol. 4, pp. S38-49, Mar 2007.

[5] G. S. Brindley, "Sensations produced by electrical stimulation of the occipital poles of the cerebral hemispheres, and their use in constructing visual prostheses," *Ann R Coll Surg Engl,* vol. 47, pp. 106-8, Aug 1970.

[6] W. H. Dobelle and M. G. Mladejovsky, "Phosphenes produced by electrical stimulation of human occipital cortex, and their application to the development of a prosthesis for the blind," *J Physiol,* vol. 243, pp. 553-76, Dec 1974.

[7] F. Duret, M. E. Brelen, V. Lambert, B. Gerard, J. Delbeke, and C. Veraart, "Object localization, discrimination, and grasping with the optic nerve visual prosthesis," *Restor Neurol Neurosci,* vol. 24, pp. 31-40, 2006.

[8] R. A. Normann, E. M. Maynard, P. J. Rousche, and D. J. Warren, "A neural interface for a cortical vision prosthesis," *Vision Research,* vol. 39, pp. 2577-87, Jul 1999.

[9] H. Kanda, T. Morimoto, T. Fujikado, Y. Tano, Y. Fukuda, and H. Sawai, "Electrophysiological studies of the feasibility of suprachoroidal-transretinal stimulation for artificial vision in normal and RCS rats," *Invest Ophthalmol Vis Sci,* vol. 45, pp. 560-6, Feb 2004.

[10] A. B. Majji, M. S. Humayun, J. D. Weiland, S. Suzuki, S. A. D'Anna, and E. de Juan, Jr., "Long-term histological and electrophysiological results of an inactive epiretinal electrode array implantation in dogs," *Invest Ophthalmol Vis Sci,* vol. 40, pp. 2073-81, Aug 1999.

[11] C. de Balthasar, S. Patel, A. Roy, R. Freda, S. Greenwald, A. Horsager, M. Mahadevappa, D. Yanai, M. J. McMahon, M. S. Humayun, R. J. Greenberg, J. D. Weiland, and I. Fine, "Factors affecting perceptual thresholds in epiretinal prostheses," *Invest Ophthalmol Vis Sci,* vol. 49, pp. 2303-14, Jun 2008.

[12] N. B. Dommel, Y. T. Wong, T. Lehmann, C. W. Dodds, N. H. Lovell, and G. J. Suaning, "A CMOS retinal neurostimulator capable of focussed, simultaneous stimulation," *J Neural Eng,* vol. 6, p. 035006, Jun 2009.

[13] Y. T. Wong, N. Dommel, P. Preston, L. E. Hallum, T. Lehmann, N. H. Lovell, and G. J. Suaning, "Retinal neurostimulator for a multifocal vision prosthesis," *IEEE Trans Neural Syst Rehabil Eng,* vol. 15, pp. 425-34, Sep 2007.

[14] R. J. Tusa, L. A. Palmer, and A. C. Rosenquist, "The retinotopic organization of area 17 (striate cortex) in the cat," *J Comp Neurol,* vol. 177, pp. 213-35, Jan 15 1978.

[15] T. L. Rose and L. S. Robblee, "Electrical stimulation with Pt electrodes. VIII. Electrochemically safe charge injection limits with 0.2 ms pulses," *IEEE Trans Biomed Eng,* vol. 37, pp. 1118-20, Nov 1990.

[16] L. F. Heffer and J. B. Fallon, "A novel stimulus artifact removal technique for high-rate electrical stimulation," *J Neurosci Methods,* vol. 170, pp. 277-84, May 30 2008.